



## Original Paper

# Factors influencing oil recovery by surfactant–polymer flooding in conglomerate reservoirs and its quantitative calculation method

Feng-Qi Tan <sup>a, b, \*</sup>, Chun-Miao Ma <sup>a, b, \*\*</sup>, Jian-Hua Qin <sup>c</sup>, Xian-Kun Li <sup>a, b</sup>, Wen-Tao Liu <sup>c</sup><sup>a</sup> College of Earth and Planetary Sciences, University of Chinese Academy of Sciences, Beijing, 100049, China<sup>b</sup> Key Laboratory Computational Geodynamics, Chinese Academy of Sciences, Beijing, 100049, China<sup>c</sup> Xinjiang Oilfield Company, PetroChina, Karamay, Xinjiang, 834000, China

## ARTICLE INFO

## Article history:

Received 17 February 2021

Accepted 6 December 2021

Available online 7 January 2022

Edited by Yan-Hua Sun

## Keywords:

Conglomerate reservoir

Water flooding

Surfactant–polymer flooding

Residual oil type

Influencing factor

Enhanced oil recovery

Computational model

## ABSTRACT

This study aims to clarify the factors influencing oil recovery of surfactant–polymer (SP) flooding and to establish a quantitative calculation model of oil recovery during different displacement stages from water flooding to SP flooding. The conglomerate reservoir of the Badaowan Formation in the seventh block of the Karamay Oilfield is selected as the research object to reveal the start-up mechanism of residual oil and determine the controlling factors of oil recovery through SP flooding experiments of natural cores and microetching models. The experimental results are used to identify four types of residual oil after water flooding in this conglomerate reservoir with a complex pore structure: oil droplets retained in pore throats by capillary forces, oil cluster trapped at the junction of pores and throats, oil film on the rock surface, isolated oil in dead-ends of flow channel. For the four types of residual oil identified, the SP solution can enhance oil recovery by enlarging the sweep volume and improving the oil displacement efficiency. First, the viscosity-increasing effect of the polymer can effectively reduce the permeability of the displacement liquid phase, change the oil–water mobility ratio, and increase the water absorption. Furthermore, the stronger the shear drag force of the SP solution, the more the crude oil in a porous medium is displaced. Second, the surfactant can change the rock wettability and reduce the absorption capacity of residual oil by lowering interfacial tension. At the same time, the emulsification further increases the viscosity of the SP solution, and the residual oil is recovered effectively under the combined effect of the above two factors. For the four start-up mechanisms of residual oil identified after water flooding, enlarging the sweep volume and improving the oil displacement efficiency are interdependent, but their contribution to enhanced oil recovery are different. The SP flooding system primarily enlarges the sweep volume by increasing viscosity of solution to start two kinds of residual oil such as oil droplet retained in pore throats and isolated oil in dead-ends of flow channel, and primarily improves the oil displacement efficiency by lowering interfacial tension of oil phase to start two kinds of residual oil such as oil cluster trapped at the junction of pores and oil film on the rock surface. On this basis, the experimental results of the oil displacement from seven natural cores show that the pore structure of the reservoir is the main factor influencing water flooding recovery, while the physical properties and original oil saturation have relatively little influence. The main factor influencing SP flooding recovery is the physical and chemical properties of the solution itself, which primarily control the interfacial tension and solution viscosity in the reservoir. The residual oil saturation after water flooding is the material basis of SP flooding, and it is the second-most dominant factor controlling oil recovery. Combined with the analysis results of the influencing factors and reservoir parameters, the water flooding recovery index and SP flooding recovery index are defined to further establish quantitative calculation models of oil recovery under different displacement modes. The average relative errors of the two models are 4.4% and 2.5%, respectively; thus, they can accurately predict the oil recovery of different displacement stages and the ultimate reservoir oil recovery.

© 2022 The Authors. Publishing services by Elsevier B.V. on behalf of KeAi Communications Co. Ltd. This is an open access article under the CC BY-NC-ND license (<http://creativecommons.org/licenses/by-nc-nd/4.0/>).

\* Corresponding author. College of Earth and Planetary Sciences, University of Chinese Academy of Sciences, Beijing, 100049, China.

\*\* Corresponding author. Key Laboratory Computational Geodynamics, Chinese Academy of Sciences, Beijing, 100049, China.

E-mail addresses: [tanfengqi@ucas.ac.cn](mailto:tanfengqi@ucas.ac.cn) (F.-Q. Tan), [machunmiao21@mails.ucas.ac.cn](mailto:machunmiao21@mails.ucas.ac.cn) (C.-M. Ma).

## 1. Introduction

Surfactant–polymer (SP) flooding is an important way to enhance oil recovery in old oilfields that have undergone water flooding (Olajire, 2014; Song, 2014; Yang et al., 2013). When the polymer and surfactant system, which is one combination type of displacement media in tertiary oil recovery technology, enters the porous medium, the synergistic effect of polymer and surfactant can increase the displacement liquid viscosity and reduce the oil–water interfacial tension. On the one hand, the sweep volume of the SP solution can be enlarged by changing the oil–water mobility ratio and increasing the oil-phase permeability (Rogachev and Kondrashev, 2015). On the other hand, the oil displacement efficiency of crude oil in porous media can be improved by changing the rock wettability and reducing the absorption capacity of residual oil (Shah and Schechter, 1977). Ultimately, the purpose of enhancing oil recovery is achieved by chemical flooding. SP flooding has been studied since the 1960s. First, a series of pilot experiments was performed by reservoir geologists in the United States, and good field-application results were obtained (Puerto et al., 2012; Shiran and Skauge, 2013). In the early 1990s, China successively deployed development test areas in the Daqing, Jilin, Shengli, and Changqing Oilfields and achieved good development effects and economic benefits. These results provide strong technical support for reducing water cut and increasing oil production in old oilfields that have been displaced by water flooding (Bai et al., 2015; Chen et al., 2012; Zhang et al., 2010). The above research results were presented for sandstone reservoirs with uniform pore structure. Conversely, few studies have been conducted on conglomerate reservoirs with complex pore structures due to the particularity of reservoir characteristics and the limitation of its distribution area.

A conglomerate reservoir is a special kind of clastic reservoir. Due to the nearby source, multiwater system, and rapidly changing sedimentary environment of the reservoir, its micropore structure presents complex-mode characteristics. The distribution of pores and throats is extremely uneven, with a small throat radius, large pore-to-pore throat radius ratio, and low pore throat coordination number, generally reflecting the characteristics of a multiphase pore throat distribution with small pore throats (Luo and Zhang, 1992; Tan et al., 2010). The special pore structure leads to a more complicated production characteristic of crude oil under different displacement modes. At present, the focus of SP flooding in a conglomerate reservoir is mainly on the oil displacement mechanism and profile control technology. Liu et al. performed experiments on sand-filled pipes, natural cores and micromodels to reveal the oil displacement mechanism of SP solution by enlarging the sweep volume and improving the oil displacement efficiency (Liu et al., 2017). Zhang et al. used a microetching model to clarify the oil displacement mechanism of SP solution by emulsification on displacing five types of residual oil after water flooding (Zhang et al., 2020). Liu et al. designed a natural core-displacement experiment to determine the effects of different micropore structures on enhanced oil recovery by SP flooding (Liu et al., 2020). Chen and Nie proposed a profile-control technology using an “expanded particle + strong gel” system to block the high permeability channel and “medium-weak gel” to adjust the permeability difference of a reservoir, ensuring the development effect of SP flooding (Chen and Nie, 2015). However, few studies have reported the influencing factors and quantitative calculation methods of enhancing oil recovery by SP flooding in conglomerate reservoirs.

In the Xinjiang Oilfield, the geological reserves of medium-high permeability conglomerate reservoirs suitable for SP flooding reach 203 million tons, and the newly increased recoverable reserves are expected to be 26.175 million tons (Li et al., 2017), showing great

development potential with SP flooding. In 2008, a major development test of SP flooding has been performed in the Kexia Formation of the seventh block to explore methods and gain experience. The large-scale SP flooding has been performed in the Badaowan Formation of the 530 well block and the Kexia Formation in the seventh block since 2015, and an obvious application effect has been achieved. However, with the development of chemical flooding in conglomerate reservoirs, some basic geological problems are also emerging gradually. Among them, the influencing factors and quantitative calculation methods of SP flooding recovery urgently need to be clarified and established. Therefore, according to the development status of the conglomerate reservoir in the Badaowan Formation of the seventh block, full-diameter conglomerate cores are selected to design the oil displacement experiments of microtransparent simulations and natural cores. On the basis of clarifying displacement mechanism of the SP solution in the conglomerate reservoir with a complex structure, the factors influencing oil recovery are determined, and quantitative calculation models of oil recovery of water flooding and SP flooding are then established. The research results can provide a geological basis and technical support for the optimization of development program by SP flooding.

## 2. Geological background of reservoir

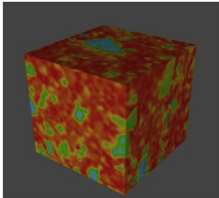
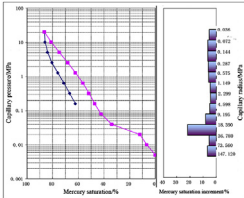
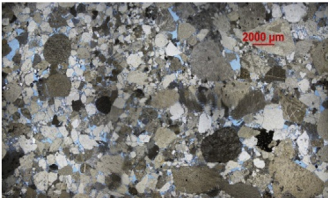
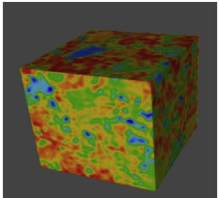
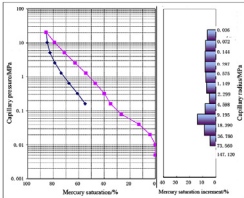
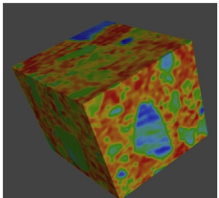
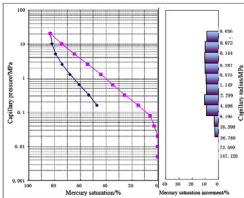
The Badaowan Formation of the seventh block in the Karamay Oilfield is located in the middle part of the Ke-Wu Fault Belt in the northwest margin of the Junggar Basin. It is cut by the Ke-Wu Fault and southern Baijiantan Fault and distributed in a strip along the fault, the structural characteristic forms a monocline inclined to the southeast and southwest, gradually steepening along the dip direction. On the whole, it belongs to a structural-lithologic reservoir. The Badaowan Formation includes five sand layers such as  $J_1b_5$ ,  $J_1b_4$ ,  $J_1b_3$ ,  $J_1b_2$  and  $J_1b_1$  from bottom to top. Among them, layer  $J_1b_5$  is a set of gravelly braided river sedimentary systems, primarily developed braided channel and mid-channel bar microfacies, which is the target layer of SP flooding (Wang et al., 2012). Sealed core data show that the average porosity and permeability of the reservoir are 18.1% and 134.2 mD, respectively, indicating that it is a conglomerate reservoir with medium porosity and medium-high permeability. The main oil-bearing lithologies in the Badaowan Formation of the seventh block are pebbly gritstone, sandy conglomerate and conglomerate. The reservoir is characterized by rapidly changing lithology and serious heterogeneity, the micro pore structure of several lithologies presents complex mode characteristics (Table 1). The pore types are mainly intergranular dissolved pores and primary intergranular pores, and the throat types are mainly necking-shaped throats and sheet-shaped pore throats, with diameters ranging from 10 to 20  $\mu\text{m}$ . The reservoir was discovered in 1959 and has been developed by water flooding for more than 50 years. At present, an adjustment program of SP flooding is being prepared. The determination of the influencing factors and the establishment of a quantitative calculation model of SP flooding recovery are the keys to achieve the design goal of this chemical flooding.

## 3. Experimental methods and procedures

### 3.1. Preparation of cores and microetching model

Due to the strong heterogeneity of conglomerate reservoirs and the complex characteristics of their pore structures, seven full-diameter conglomerate cores, which were collected from the Badaowan Formation reservoir in the seventh block of the Karamay Oilfield, were used to prepare experimental core samples to reduce

**Table 1**  
Characteristics of the micropore structures of different lithologies in the studied conglomerate reservoir.

| Lithology          | Core photos   | Casting thin section  | 3D pore distribution   | Capillary pressure curve  |
|--------------------|---|---|--|---|
| Pebbly gritstone   |  |  |  |  |
| Sandy conglomerate |  |  |  |  |
| Conglomerate       |  |  |  |  |

the influence of core size on oil displacement. Among the samples, two are pebbly gritstone samples (SP-2, SP-7), two are conglomerate samples (SP-4, SP-5), and three are sandy conglomerate samples (SP-1, SP-3, SP-6), representing the main oil-bearing lithologies of the reservoir (Fig. 1).

The core samples were cut from the full-diameter conglomerate cores with a diameter of 12 cm and a length of 15 cm to fit the core holder size of the flooding system. Then, the three-dimensional (3D) distribution characteristics of the micropore structure of the seven core samples were reconstructed by CT scanning to create a reference model of the distribution of pores and pore throats for the microetching model.

The microscopic model was prepared to simulate the natural cores according to the 3D pore-throat distribution map formed by CT scanning and the photolithographic method, the pore network in the cast thin section was reproduced by the photoetching method, and a micromodel was generated for visual simulation. The dimensions of the microetching model were 85.0 mm × 85.0 mm × 4.0 mm with the pore diameters of 1.0–90 μm, and holes were included at both sides of the model to simulate the injection well and production well.

### 3.2. Experimental materials and instruments

The brine used was the formation water taken from the Badaowan Formation reservoir and its properties and composition are listed in Table 2. The crude oil used was from the same reservoir and its properties are listed in Table 3.

Partially hydrolyzed polyacrylamide (HPAM), a water-soluble polymer, was provided by Beijing Hengju Chemical Co., Ltd., with a relative molecular weight of  $1500 \times 10^4$  and a hydrolysis of 25.5%. Petroleum sulfonate (KPS, a surfactant) was obtained from Beijing Xingmeiya Chemical Co., Ltd., with an active mass fraction of 15%. The composition of SP flooding system is different for 7 different core samples, the purpose is to determine the main factors of

affecting the oil recovery of conglomerate reservoir in the process of SP flooding. The composition and parameters of SP systems are listed in Table 4.

The rotary drop interfacial tensiometer with the model number of TX-500B was used to measure the interfacial tension of different SP systems. A full-diameter core displacement device with the model number of Quizix SP-5000 was used to hold seven core samples of standard size for SP flooding experiment. In the process of oil displacement, a LIGHTSPEED 8-slice spiral CT instrument produced by GE company in the United States was used to scan the distribution characteristics of oil and water in rock cores under different pore volume values. After water flooding and SP flooding, the ultraviolet fluorescence microscope with the model number of Olympus CX23 was used to effectively analyze the occurrence state of residual oil.

### 3.3. Analysis of micropore structure characteristics

The data of physical properties and constant-rate mercury injections from seven core samples show that the average values of original porosity and original gas permeability of Badaowan Formation reservoir are 19.4% and 199.3 mD, respectively, indicating that it is a conglomerate reservoir with medium porosity and medium-high permeability. The micro pore structure presents complex mode characteristics as a whole, the pore types are mainly intergranular dissolved pores and primary intergranular pores, with capillary radius from 4 to 11 μm and its average value of 7.50 μm. The throat types are mainly necking-shaped throats and sheet-shaped pore throats, with throat radius from 7 to 20 μm and its average value of 12.84 μm (Table 4).

### 3.4. Natural core samples

The injection water, polymer and surfactant were mixed in different proportions to formulate SP solutions with different

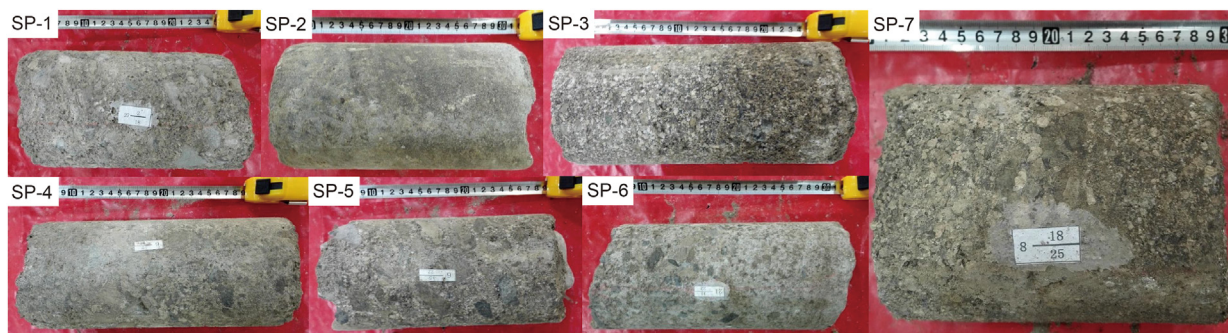


Fig. 1. Lithologic characteristics of experimental core samples (SP-2 and SP-7 are pebbly gritstone; SP-1, SP-3 and SP-6 are sandy conglomerate; SP-4/SP-5 are conglomerate).

Table 2  
Properties and composition of formation water.

| Type               | Salinity, mg·L <sup>-1</sup> | pH   | Ion concentration, mg·L <sup>-1</sup> |                               |                               |                                 |                  |                  |
|--------------------|------------------------------|------|---------------------------------------|-------------------------------|-------------------------------|---------------------------------|------------------|------------------|
|                    |                              |      | Cl <sup>-</sup>                       | HCO <sub>3</sub> <sup>-</sup> | SO <sub>4</sub> <sup>2-</sup> | Na <sup>+</sup> +K <sup>+</sup> | Mg <sup>2+</sup> | Ca <sup>2+</sup> |
| NaHCO <sub>3</sub> | 9810.4                       | 7.48 | 4090.7                                | 2250.2                        | 5.1                           | 3358.2                          | 32.6             | 73.6             |

Table 3  
Properties and compositions of crude oil.

| Density, g·cm <sup>-3</sup> | Viscosity, mPa·s | Acid, mg·L <sup>-1</sup> | SARA composition, % |           |        |             |
|-----------------------------|------------------|--------------------------|---------------------|-----------|--------|-------------|
|                             |                  |                          | Saturates           | Aromatics | Resins | Asphaltenes |
| 0.842                       | 28.5             | 0.293                    | 48.47               | 6.85      | 41.95  | 2.63        |

Table 4  
Parameters of the oil displacement experiments of natural cores.

| Core number | SP solution                | Interfacial tension, mN·m <sup>-1</sup> | Gas permeability, mD | Porosity, % | Original oil saturation, % | Throat radius, μm | Average capillary radius, μm |
|-------------|----------------------------|---|----------------------|-------------|----------------------------|-------------------|------------------------------|
| SP-1        | 1500 mg/L HPAM + 0.05% KPS | 0.925                                   | 295                  | 21.4        | 65.5                       | 9.60              | 9.69                         |
| SP-2        | 1500 mg/L HPAM + 0.1% KPS  | 0.00802                                 | 128                  | 19.9        | 64.3                       | 7.73              | 8.35                         |
| SP-3        | 1500 mg/L HPAM + 0.2% KPS  | 0.0041                                  | 149                  | 21.9        | 64.4                       | 10.13             | 10.57                        |
| SP-4        | 1500 mg/L HPAM + 0.1% KPS  | 0.00802                                 | 20.0                 | 18.3        | 60.3                       | 19.91             | 6.31                         |
| SP-5        | 1500 mg/L HPAM + 0.2% KPS  | 0.0041                                  | 37.1                 | 15.4        | 60.3                       | 7.17              | 4.31                         |
| SP-6        | 1000 mg/L HPAM + 0.1% KPS  | 0.004                                   | 227                  | 21.1        | 62.4                       | 19.91             | 7.02                         |
| SP-7        | 1000 mg/L HPAM + 0.1% KPS  | 0.004                                   | 539                  | 17.9        | 61.5                       | 15.45             | 6.22                         |

viscosity ratios and interfacial tensions by adjusting the concentration of the polymer and surfactant. In addition, the porosity, permeability and micropore structural parameters of seven natural cores were determined using the constant-rate mercury injection curve of different lithologies (Table 4), which provided basic data for the analysis of factors influencing the recovery of water flooding and SP flooding.

The experimental procedures are as follows.

- (1) After washing oil and salt by solution extraction method, the core sample was dried in an oven at 60 °C for 48 h and then its dimensions were measured with an electronic digital caliper and recorded.
- (2) The core sample was vacuumed for 3 h and then saturated with formation water until the water drained continuously at the outlet of the core.
- (3) The core sample was saturated with crude oil at a rate of 0.02 mL/min at 30 °C (reservoir temperature) until no water was produced (i.e. the volume of water in the metering tube no longer increased within 2 h). The volume of oil injected into the core sample was recorded and the original oil

saturation was calculated (Table 4). The oil-saturated core sample was scanned by *in situ* CT.

- (4) Displacement water was injected into the core at a rate of 0.01 mL/min, which was determined according to the injection rate in the oilfield. Water injection continued until the water cut of the fluids produced at the outlet reached 98%. In the water injection process, the core sample was scanned by *in situ* CT at different pore volume (PV) values of water injection to determine the oil and water distribution characteristics, and the volumes of water and oil produced at the core outlet were simultaneously recorded in real time. Then the water cut, oil recovery and displacement pressure at different displacement times were calculated.
- (5) After water flooding, the SP system was injected into the core sample at a rate of 0.01 mL/min. SP flooding was stopped when the water cut at the outlet reached 98%. In this process, the sample was scanned by *in situ* CT at different injection volumes of the SP system, and also the volumes of water and oil produced were simultaneously recorded. The water cut, oil recovery and displacement pressure at different displacement times were calculated.

### 3.5. Displacement in imcromodel (microscopic model)

The optimized formula of the SP system was composed of 1500 mg/L HPAM (15 million) + 0.2% KPS, and its interfacial tension was 0.0046 mN/m.

The experimental procedures are as follows.

- (1) The microetching model was vacuumed for 3 h and saturated for 24 h with formation water, which was taken from the Badaowan Formation in the seventh block.
- (2) The formation water was displaced with crude oil and kept in a stable state for 24 h.
- (3) Displacement water was injected into the core at a rate of 0.001 mL/min until the water cut reached 98%, resulting in only the residual oil caused by water flooding in the model.
- (4) The SP solution was injected to displace the residual oil after water flooding at a rate of 0.001 mL/min, and the displacement process was recorded by video technology. Then, the oil displacement mechanisms of the SP flooding and the production of crude oil in porous media were analyzed (Fig. 2).

### 3.6. Determination of the residual oil type after water flooding

To determine the type of residual oil left in the water-flooded conglomerate reservoir and to clarify the displacement mechanisms of the residual oil by SP flooding, the distribution of residual oil was observed with the ultraviolet fluorescence microscope based on frozen-core slice-grinding technology.

The experimental procedure is as follows.

- (1) A water flooding experiment was performed on natural cores until the water cut at the outlet reached 98%.
- (2) The core was frozen with liquid nitrogen and then sliced.
- (3) The slices were ground to a thickness of 0.1 mm to improve the observation accuracy of the residual oil.
- (4) The ground slices were observed under the ultraviolet fluorescence microscope to effectively distinguish the rock, oil and water, and then the occurrence types of the residual oil were determined.

## 4. Results and discussion

### 4.1. Types of residual oil after water flooding

Due to differences of the viscous-elastic behavior between water and SP solution, the percolation characteristics of water are different from those of SP solution when they enter the microscopic pores. This results in different distributions of residual oil (Xu et al., 2011; Liu et al., 2016).

To clarify the displacement mechanisms of the SP system for the residual oil remaining after water flooding and analyze the contribution of different types of residual oil to enhanced oil recovery by SP flooding, it is necessary to determine the main distribution forms of residual oil trapped in the conglomerate reservoir after water flooding. An ultraviolet fluorescence microscopy technique has been developed to visualize the oil distribution in oil reservoirs. Direct observations of pictures taken by the ultraviolet fluorescence microscope indicate that four types of residual oil were identified in the water-flooded conglomerate reservoir: (1) oil droplets retained in pore throat by capillary forces, (2) oil cluster trapped at the junction of pores and throats, (3) oil film on the rock surface, and (4) isolated oil in dead-ends of flow channel. Based on the fluorescence areas of different types of residual oil and the total residual oil, the proportion of each type of residual oil was calculated. The calculation results show that the oil droplets and oil cluster are the main types of residual oil trapped in the reservoir, accounting for 52.4% and 30.8%, respectively, whereas oil film and isolated oil accounting for 10.5% and 6.3%, respectively.

The formations of different types of residual oil after water flooding are different. Oil droplets retained in pore throats primarily exist between rock particles because of capillary forces. Due to the existence of dominant flow channels in micropores and the higher permeability of the water phase than that of the oil phase, the crude oil stored in a small pore throat cannot be swept effectively, the larger capillary force make the oil droplets retain in the pore throat to form this type of residual oil (Fig. 3a). Oil cluster primarily exists at the junction of pores and throats. Due to the difference in the pore sizes and the change in the solution flow rates, the oil droplets flowing with displacement fluid during water flooding easily cluster in microscopic pores to form this type of residual oil (Fig. 3b). The thin oil film is formed primarily due to the surface adsorption of clay particles or mineral particles. The viscosity of injection water is relatively low and cannot change rock wettability in a short time, so in the main channels of water flooding, the oil adsorbed on the rock surface is not displaced out and then oil film is formed (Fig. 3c). Isolated oil exists in dead-ends of complex flow channel because the dead end has no seepage capacity, the displacement liquid cannot pass through, and oil accumulates under the Jamin effect, forming isolated oil in dead-ends (Fig. 3d). The effective displacement of the four types of residual oil is the material basis of enhancing oil recovery by SP flooding.

### 4.2. Microdisplacement mechanism of SP flooding

Based on the determination of types of residual oil in the conglomerate reservoir after water flooding, the microetching model was used to study the displacement mechanisms of the SP solution and reveal the start-up mechanism of different types of

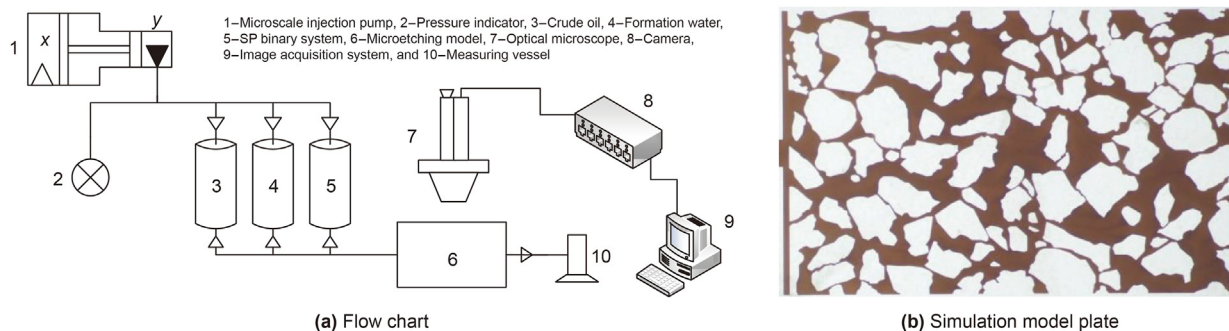


Fig. 2. Flow chart and simulation plate of the microetching model experiment.

residual oil, which provides a geological basis for the accurate prediction of SP flooding recovery.

#### 4.2.1. Displacement mechanism of oil droplets retained in pore throat

For oil droplets retained in pore throat by capillary forces, when the SP solution flows through the pore throat, the change in the oil–water mobility ratio prevents the displacement fluid from “fingering forward” along the dominant flow channel of water flooding. Under the effect of an increased viscosity, the front edge of some SP solutions enters the pores, displacing the crude oil that cannot be displaced by injection water. The oil droplets retained in pore throats largely form along a flow channel. When the SP solution completely enters the intergranular pores, surfactants can change the rock wettability and reduce the oil–water interfacial tension. Under the stripping of high-viscosity displacement fluid, the crude oil is separated into droplets or filaments, which are then removed by the solution. In addition, surfactants in porous media can emulsify crude oil, especially the residual oil adsorbed on the pore throat wall. After emulsification, the adsorption capacity of the residual oil is reduced, and the viscosity of the displacement fluid can be further increased. Through the interaction of the above two factors, the oil droplets retained in pore throat are stripped and displaced, further improving the oil displacement efficiency (Fig. 4).

#### 4.2.2. Displacement mechanism of oil cluster trapped at the junction of pores and throats

The water flooding results show that oil cluster is primarily distributed at the junction of pores and pore throats. When the SP solution flows to oil cluster trapped in the microscopic pores, the phase permeability of the displacement fluid decreases and that of the crude oil in the porous media increases due to the viscosity-increasing effect of the polymer. The change in the oil–water mobility ratio makes the SP solution finger advance along the path with minimum resistance inside oil cluster. A series of flow channels is formed by displacing part of the crude oil, and then the surfactant can contact with the crude oil in the flow channels. Due to the resulting low-interfacial tension, the crude oil is emulsified layer by layer, and the solution viscosity further increases; thus, the residual oil is continuously stripped off, carried and displaced in the form of droplets, filaments or spots. Owing to the large contact area between the oil cluster and the SP solution, the surfactant changes the rock wettability, reduces the oil–water interfacial tension, and thus allows the SP fluid to enter crude oil between rock particles through the viscosity-increasing effect of the polymer and displace the residual oil with a stronger shear drag force, consequently improving the oil displacement efficiency (Fig. 5).

#### 4.2.3. Displacement mechanism of oil film on the rock surface

Oil film is generally adsorbed on the surface of mineral particles, especially clay mineral particles. When the SP solution comes into contact with oil film along the displacement direction, the

viscosity-increasing effect of the polymer can change the oil–water mobility ratio so that the displacement liquid starts to shear and drag oil film toward the displacement direction. When a certain volume of oil droplets aggregates, their adsorption capacity weakens, and the droplets are then cut off by the SP solution with high viscosity and displaced away (Fig. 6). As the oil film is gradually peeled off, some small gaps appear between the oil film and the particles. When the SP solution infiltrates, the surfactant changes the rock wettability from lipophilic to hydrophilic, and the low interfacial tension weakens the adsorption capacity of the oil film, which is stripped off the particles by the displacement fluid. With continuous emulsification and stripping, the oil film is completely displaced, and the oil displacement efficiency is significantly improved.

#### 4.2.4. Displacement mechanism of isolated oil in dead-ends of flow channel

Isolated oil primarily occurs in dead-ends of complex flow channels, and water flooding cannot sweep effectively without flow channels. Compared with water flooding, in the process of SP flooding, the viscosity-increasing effect of the polymer changes the oil–water mobility ratio, which causes the SP to form a displacement front in dead-ends of flow channel. Furthermore, the surfactant induces the crude oil in dead-ends of flow channels to form an emulsion due to the low interfacial tension, which further increases the viscosity of the displacement fluid. A solution with a higher viscosity carries and displaces the emulsified oil droplets or oil filaments, enlarges the sweep volume of the SP flooding system and improves the oil displacement efficiency. Finally, the purpose of starting the residual oil in dead-ends is achieved (Fig. 7). However, because the oil in dead-ends of a semiclosed pore cannot flow, some residual oil is not displaced and remains in dead-ends of flow channel after SP flooding.

In summary, for the studied conglomerate reservoir, due to the complex pore structures, the oil displacement mechanisms of SP flooding for enhanced oil recovery are primarily controlled by the sweep volume and oil displacement efficiency. The viscosity-increasing effect of the polymer initially reduces the permeability of the displacement-liquid phase and changes the oil–water mobility ratio so that a large amount of the SP can be retained in the pores. This phenomenon can overcome the “fingering forward” of the displacement fluid along the dominant flow channel. A strong shear drag force is used to carry the crude oil in porous media, and oil recovery is enhanced by enlarging the sweep volume. Subsequently, rock wettability can be changed when the surfactant comes into contact with the residual oil. The adsorption capacity of residual oil is reduced by low interfacial tension, and the viscosity of the SP system is further increased by emulsion. The residual oil is isolated and displaced in the form of filaments, droplets, and emulsions through the interaction of the above two factors, and the oil recovery is enhanced by improving the oil displacement efficiency. Among the four start-up mechanisms of

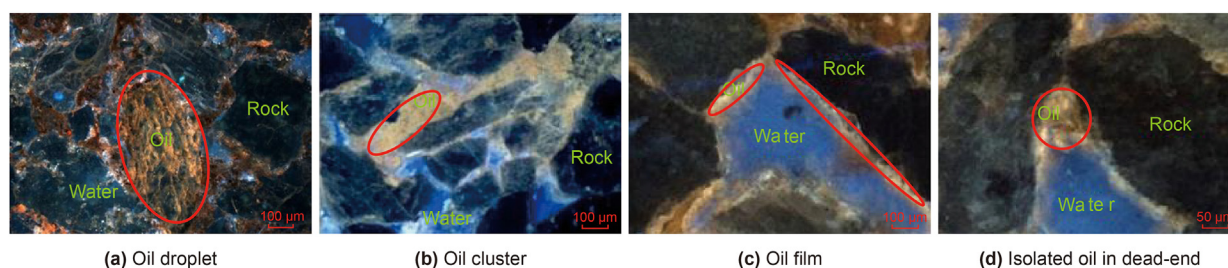


Fig. 3. Types of residual oil in the water-flooded conglomerate reservoir.

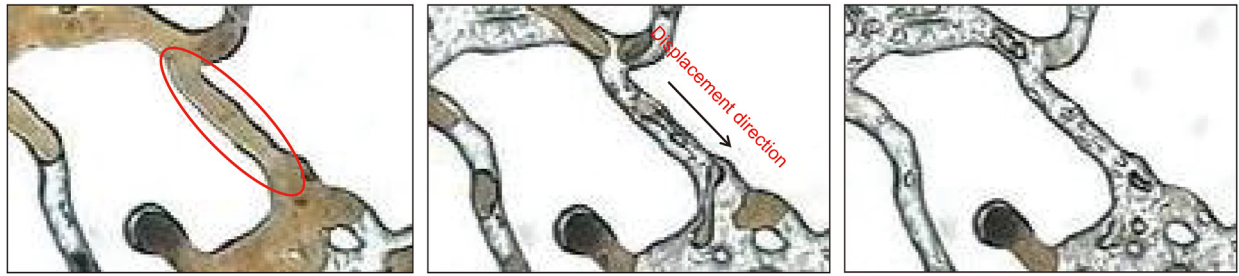


Fig. 4. Start-up mechanism of oil droplets retained in pore throats.

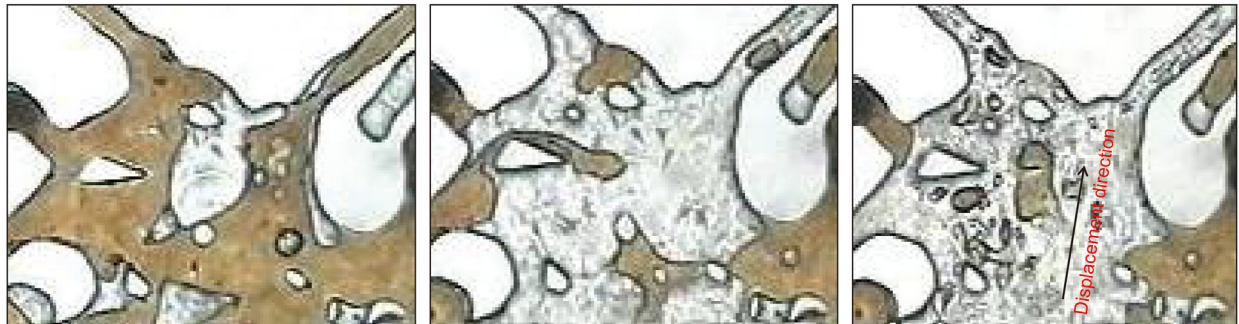


Fig. 5. Start-up mechanism of oil cluster trapped at the junction of pores and throats.

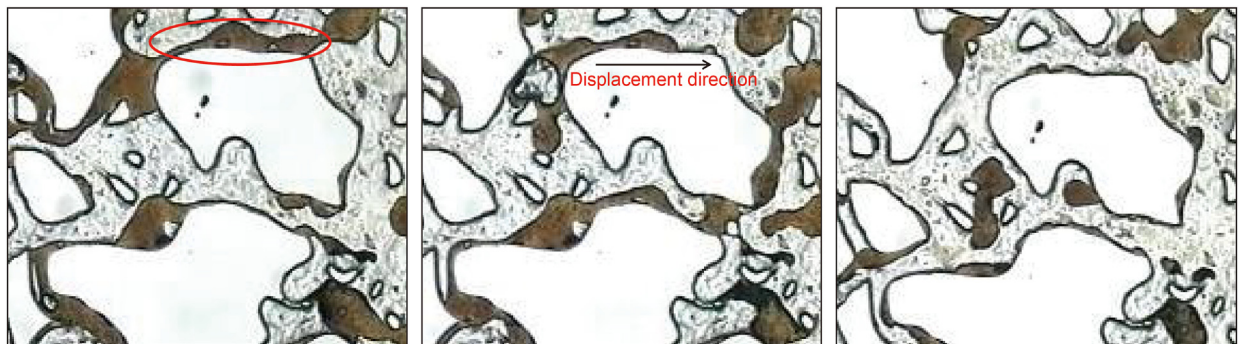


Fig. 6. Start-up mechanism of oil film on the rock surface.

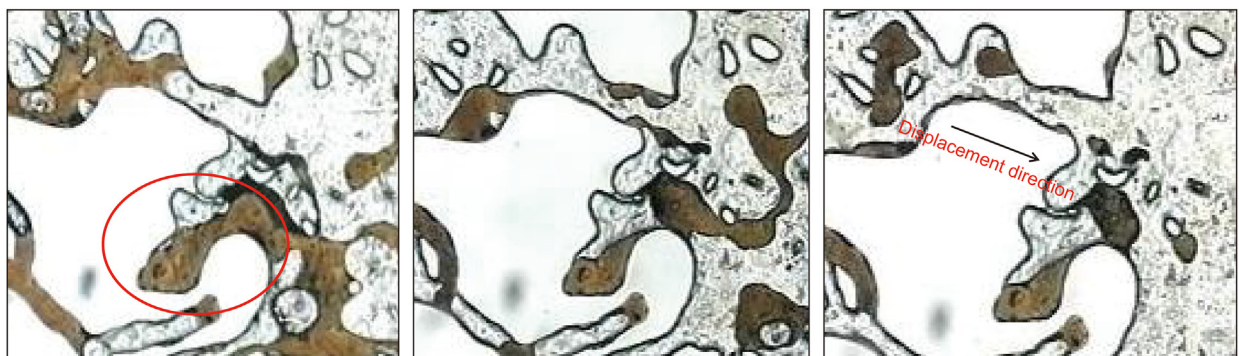


Fig. 7. Start-up mechanism of isolated oil in dead-ends of flow channel.

residual oil identified after water flooding, enlarging the sweep volume and improving the oil displacement efficiency are interdependent, but their contributions to enhanced oil recovery are different. The SP flooding system primarily enlarges the sweep

volume by increasing viscosity of solution to start two kinds of residual oil such as oil droplet retained in pore throats and isolated oil in dead-ends of flow channel, and primarily improves the oil displacement efficiency by lowering interfacial tension of oil phase to

start two kinds of residual oil such as oil cluster trapped at the junction of pores and oil film on the rock surface.

### 4.3. Influencing factors and quantitative calculation model of oil recovery

#### 4.3.1. Variation trend of oil recovery

Due to the difference in the oil displacement mechanism for different displacement media, the start-up mechanism and producing degree of crude oil in different types of micro pores and pore throats are not the same, resulting in differences in enhanced oil recovery at different displacement stages of the reservoir (Sheng, 2014; Dai et al., 2015). The experimental results of oil displacement from natural core SP-5 show that the production time of conglomerate sample in the low water cut stage is relatively short, and the initial water cut increases very quickly, the water cut of core reaches more than 95% when the volume of the water injected reaches 1 PV and it is in production stage of high water cut for a long time, the oil recovery will not be enhanced (Fig. 8). These findings indicate that a dominant flow channel is formed in the core. The sweep volume of the injection water is limited, the oil displacement efficiency is low, and the oil recovery in the water flooding stage is 36.25%. When the SP solution enters the porous medium, four types of residual oil after water flooding are started up and displaced by changing the oil–water mobility ratio and increasing the solution viscosity, the oil recovery and displacement pressure rapidly increase. Moreover, the water cut is effectively controlled and kept stable, illustrating the significant effect of SP flooding. With a continuous increase in the injection volume, the water cut of the core reaches more than 95% and it is in production stage of high water cut due to the limits of the sweep volume and oil flooding efficiency. The displacement pressure decreases, the water cut increases and remains stable, and the changing in oil recovery is small. The ultimate oil recovery of the sample is 76.53%, and the enhanced oil recovery is 40.28% with SP flooding, which is 4.03% higher than that of water flooding.

The experimental results of oil displacement from the six other natural cores show the same variation characteristics. On the whole, the production time of low water cut is relatively short due to the fast rise of water cut in the water flooding stage, resulting in a long production period with high water cut. The production time of low water cut is relatively long due to the rapid increases in oil recovery and displacement pressure and the effective control of the water cut in the SP flooding stage, resulting in a great improvement

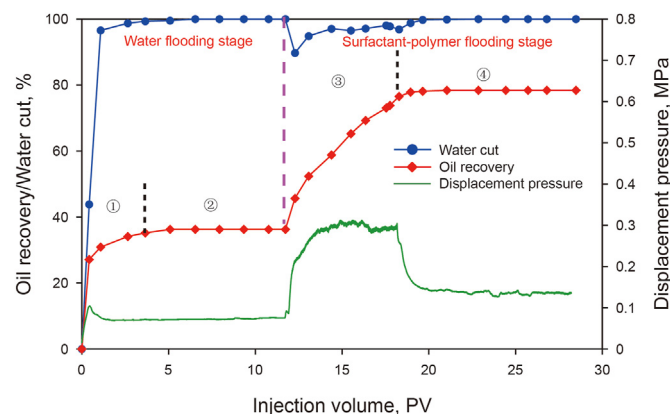


**Fig. 8.** Oil recovery change curves of water flooding and SP flooding for sample SP-5 (①/② are the stages of water flooding: ① is the effective stage of water flooding, and ② is the high water cut stage of water flooding. ③/④ are the SP flooding stages: ③ is the effective stage of SP flooding, and ④ is the high water cut stage of SP flooding).

in the ultimate oil recovery. However, due to the differences in the physical properties and pore structures of the core samples and the parameters of the SP solution, the shape and amplitude of the oil recovery curves of the water flooding and SP flooding processes of each sample are not the same (Fig. 9). Therefore, the oil recovery in different displacement stages has different influencing factors. Determining the main controlling factors of water flooding and SP flooding recovery and establishing a corresponding quantitative calculation model can provide accurate prediction parameter of oil recovery for the design of development program of SP flooding.

Generally, the factors influencing oil recovery include external factors and internal factors (Pal et al., 2018). External factors include the injection pressure, displacement rate, molecular weight of the chemical agent and solution concentration. Internal factors include the crude oil viscosity, reservoir physical properties, rock wettability and pore structure. This study primarily discusses the influence of internal factors and the interfacial tension of the SP solution on oil recovery under different displacement modes, whereas the external factors are used to determine the optimum parameter design according to experimental results. Based on the experimental displacement results of the seven natural cores and the pore structure parameters obtained from the corresponding constant-velocity mercury injection curves, the analysis data set of factors influencing oil recovery is established. Table 5 shows that the interfacial tensions of the SP solution for each sample are different, whereas the reservoir physical properties, original oil saturation and pore structure parameters are greatly different. Through the interaction of the above factors, obvious differences arise in the range of enhanced oil recovery results under different displacement modes.

#### 4.3.2. Controlling factors and calculation model of water flooding recovery

For conglomerate reservoirs, previous water-displacement mechanism experiments (Tan et al., 2019; Deng et al., 2014) have shown that the crude oil of hydrophilic rocks is primarily flooded by the “creeping” displacement of the injection water along the rock surfaces. The complex pore structure and “thin-non-network” flow pattern lead to considerable reservoir heterogeneity and a large displacement-resistance effect, thereby leaving residual oil in small pore throats, at the intersection of pores or in large pores surrounded by small pores. However, the water flooding of lipophilic rocks is dominated by “fingering forward” flow. When the injection water enters the pores, it fingers along the central part of the pores to displace crude oil, and then an oil film is formed on the pore surface due to the lipophilicity of rocks and the limitation of the viscosity of the displacement fluid. Therefore, the residual oil after water flooding is primarily distributed along the particle surfaces in the form of an oil film or occurred in small pore throats with large capillary pressure and dead-ends of flow channel. The water flooding mechanisms of hydrophilic rocks and lipophilic rocks in conglomerate reservoirs are completely different. However, the occurrence characteristics of residual oil after water flooding are closely related to the pore structure. Therefore, the water flooding recovery is affected by not only the physical properties and original oil saturation of the reservoir but also its pore structure.

Through the analysis of the relationship between the water flooding recovery and the physical properties, original oil saturation and pore structure parameters from the seven natural core samples, the correlation between water flooding recovery and average capillary radius was found to be the best, followed by that of the original oil saturation and effective porosity (Fig. 10). Therefore, under the premise of certain external injection conditions, for conglomerate reservoirs, the complex pore structure is

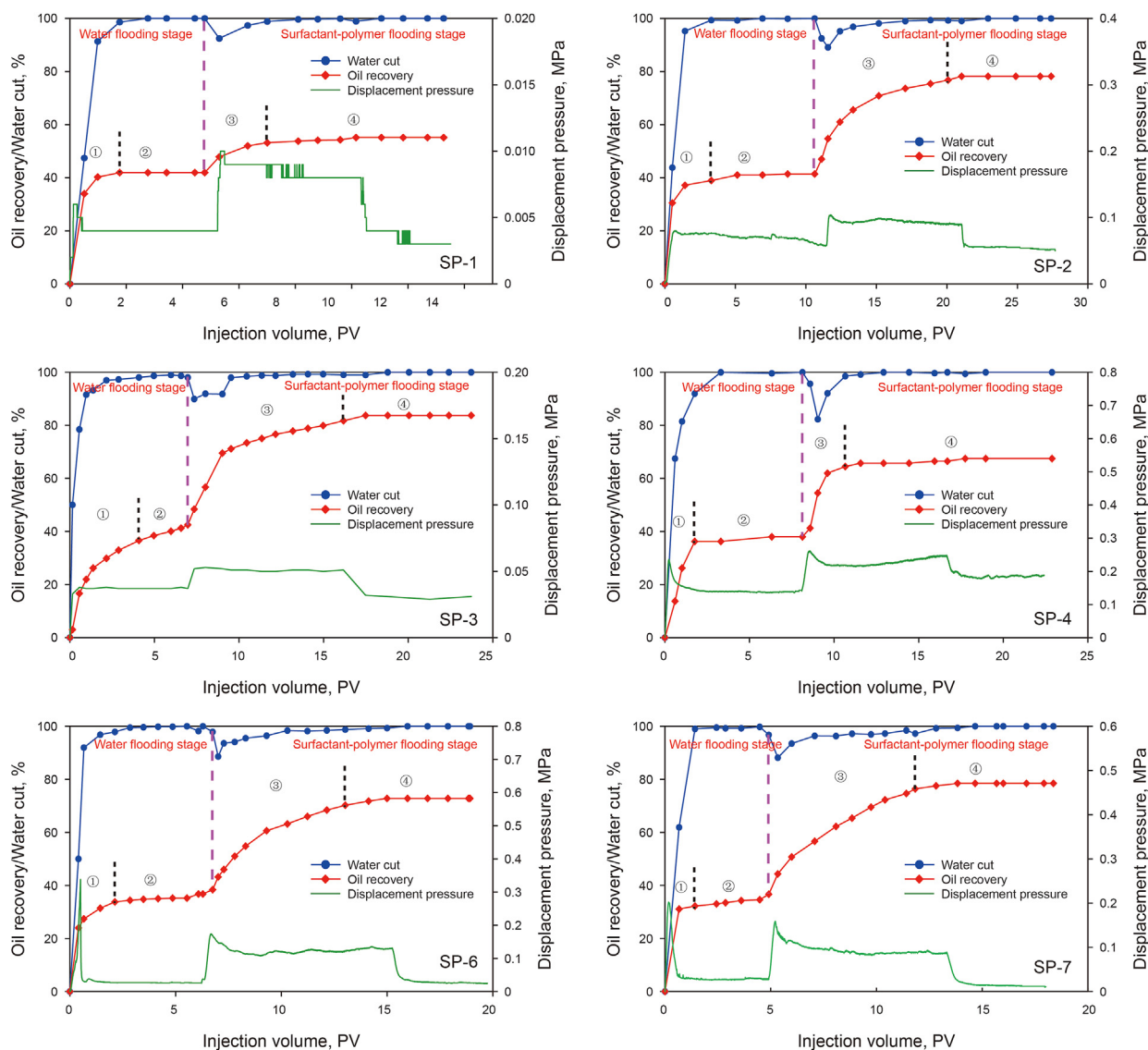


Fig. 9. Oil recovery change curves of water flooding and SP flooding for conglomerate samples.

Table 5  
Analysis data of factors influencing oil recovery under different displacement modes.

| Core number | Interfacial tension, mN/m | Permeability, mD | Porosity, % | Original oil saturation, % | Pore throat Radius, $\mu\text{m}$ | Average capillary radius, $\mu\text{m}$ | Water flooding oil recovery, % | SP flooding oil recovery, % |
|-------------|---------------------------|------------------|-------------|----------------------------|-----------------------------------|---|--------------------------------|-----------------------------|
| SP-1        | 0.925                     | 295              | 21.4        | 65.5                       | 9.60                              | 9.69                                    | 41.92                          | 12.35                       |
| SP-2        | 0.00802                   | 128              | 19.9        | 64.3                       | 7.73                              | 8.35                                    | 41.40                          | 35.44                       |
| SP-3        | 0.0041                    | 149              | 21.9        | 64.4                       | 10.13                             | 10.57                                   | 42.48                          | 39.23                       |
| SP-4        | 0.00802                   | 20.0             | 18.3        | 60.3                       | 19.91                             | 6.31                                    | 38.00                          | 28.50                       |
| SP-5        | 0.0041                    | 37.1             | 15.4        | 60.3                       | 7.17                              | 4.31                                    | 36.25                          | 40.28                       |
| SP-6        | 0.004                     | 227              | 21.1        | 62.4                       | 19.91                             | 7.02                                    | 36.80                          | 35.00                       |
| SP-7        | 0.004                     | 539              | 17.9        | 61.5                       | 15.45                             | 6.22                                    | 36.68                          | 40.83                       |

the main controlling factor affecting the water flooding efficiency, i.e., the microscopic flow system composed of pores and pore throats controls the ultimate oil recovery of water flooding. To recover the crude oil in porous media by water flooding, a higher porosity and oil saturation of the reservoir results in a greater amount of oil displaced; however, the volume of oil that can be effectively displaced is controlled by the micropore structure. Therefore, the influence of the physical properties of the reservoir

and its original oil saturation on the water flooding recovery is less than that of the pore structure.

Based on the above analysis, the main factors affecting the water flooding recovery of hydrophilic and lipophilic conglomerate reservoirs are the micropore structure of the reservoir, followed by that of the original oil saturation and effective porosity. To characterize the comprehensive influence of these three parameters on water flooding recovery, a water flooding recovery index is

constructed to quantitatively calculate the oil recovery of water flooding. The calculation formula is as follows:

$$I_w = r \frac{S_o}{\phi} \tag{1}$$

where  $I_w$  is the water flooding recovery index, dimensionless;  $r$  is the average capillary radius of the reservoir,  $\mu\text{m}$ ;  $S_o$  is the original oil saturation%;  $\phi$  is the effective porosity, %.

The water flooding recovery index reflects the original oil saturation, effective pore and micropore structures of the reservoir. Its physical meaning is the capillary radius of a pore occupied by oil saturation under a unit porosity, i.e., the pore size corresponding to residual oil. A larger water flooding recovery index means that a greater amount of crude oil is able to flow through the porous medium effectively. Under the condition of constant external displacement factors, a greater reduction in the oil saturation with water flooding corresponds to a higher water flooding recovery. Fig. 11 shows that water flooding recovery increases with an increased water flooding recovery index for each of the seven natural conglomerate samples, and there is a linear positive correlation of the results, with a good correlation. Therefore, this parameter can be used to accurately predict the oil recovery of conglomerate reservoirs in the water flooding stage. The calculation formula is as follows:

$$\begin{aligned} f_w &= 0.695I_w + 29.172 \\ R^2 &= 0.9304 \end{aligned} \tag{2}$$

where  $f_w$  is the water flooding recovery, %.

### 4.3.3. Controlling factors and calculation model of SP flooding recovery

For the four types of residual oil in the conglomerate reservoir after water flooding, the SP solution can enhance oil recovery by enlarging the sweep volume and improving the oil displacement efficiency. The viscosity-increasing effect of the polymer can effectively reduce the permeability of the displacement fluid, change the oil–water mobility ratio, increase the water absorption, and control the “fingering forward” displacement of the injection solution. Thus, crude oil in porous media can be displaced by a strong shear drag force. In addition, the surfactant can also change rock wettability, reduce the adsorption capacity of residual oil by lowering the interfacial tension, and further increase the viscosity of the SP solution by emulsification. Under the combined effect of the above two factors, residual oil is recovered. Therefore, the micro displacement mechanism of SP flooding is completely different

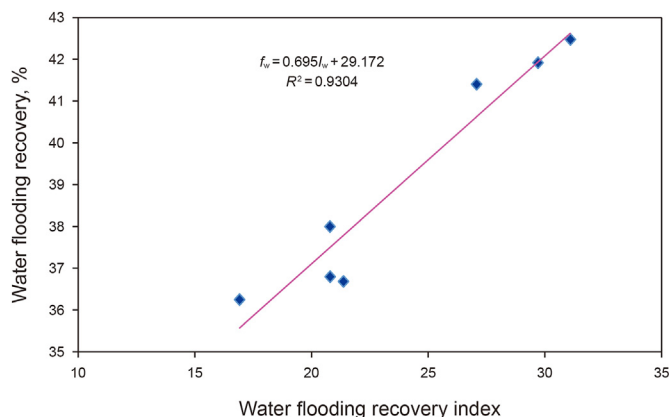


Fig. 11. Crossplot of water flooding recovery and water flooding recovery index.

from that of water flooding, so the controlling factors of oil recovery are also different.

Through the analysis of the relationship between the SP flooding recovery and the physical properties, residual oil saturation after water flooding, pore structure parameters from the seven natural core samples and SP solution parameters, the pore structure was identified as the main controlling factor affecting the oil recovery of water flooding. However, due to the difference in oil displacement mechanisms between the primary and secondary flooding processes, the pore structure is no longer the main controlling factor of SP flooding, and the correlation between the enhanced oil recovery of SP flooding and the two parameters of porosity and average capillary radius is not as high as that of water flooding. However, the interfacial tension, solution viscosity and residual oil saturation after water flooding have good correlations with the enhanced oil recovery of SP flooding. In particular, the solution viscosity and interfacial tension have the highest degree of coincidence (Fig. 12). Thus, the physical and chemical properties of the solution are the main factors affecting SP flooding recovery. When the displacement fluid comes into contact with the residual oil after water flooding along a flow channel in porous media, the crude oil can be produced by changing the oil–water mobility ratio and reducing the oil–water interfacial tension, thereby enhancing oil recovery. Furthermore, the higher residual oil saturation after water flooding means that the volume of crude oil that can be displaced by the SP solution is larger, under the premise of the same SP solution formula, enhancing oil recovery is also higher by SP flooding.

The above analysis demonstrates that the main factors affecting SP flooding recovery are interfacial tension, solution viscosity and residual oil saturation. To characterize the comprehensive influence of these three parameters on SP flooding recovery, the SP flooding recovery index is constructed to quantitatively calculate the oil recovery of SP flooding. The calculation formula is as follows:

$$I_{sp} = \frac{\mu S_{wo}}{\gamma} \tag{3}$$

where  $I_{sp}$  is the SP flooding recovery index, dimensionless;  $\mu$  is the solution viscosity,  $\text{mPa}\cdot\text{s}$ ;  $\gamma$  is the interfacial tension,  $\text{mN/m}$ ;  $S_{wo}$  is the residual oil saturation after water flooding.

The enhanced oil recovery of SP flooding is closely related to the residual oil saturation, interfacial tension and solution viscosity. The residual oil saturation is the material basis of SP flooding. Only when the residual oil saturation after water flooding is higher, the SP flooding solution can play better its chemical flooding effect by

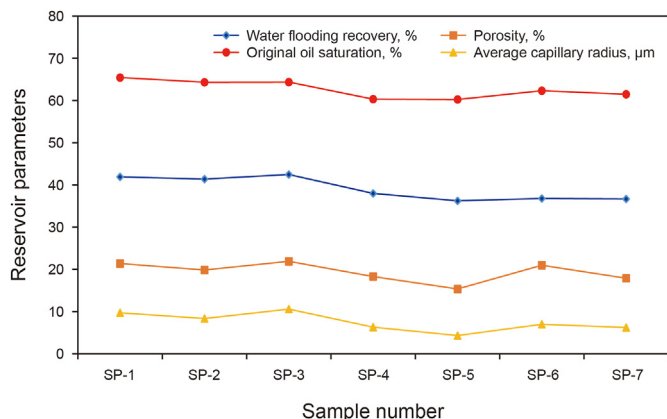


Fig. 10. Relationship between water flooding recovery and influencing factors.

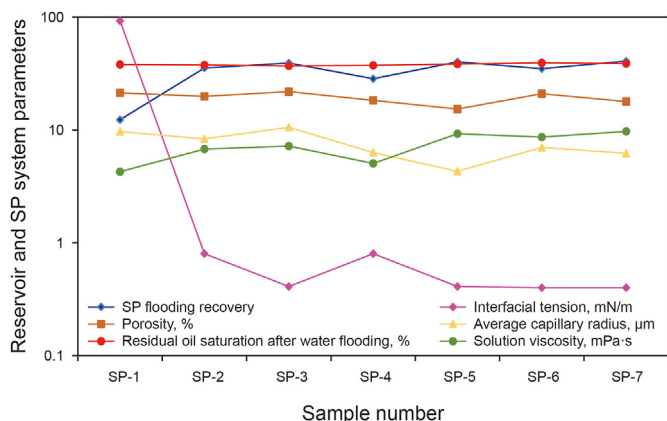


Fig. 12. Relationship between SP flooding recovery and influencing factors.

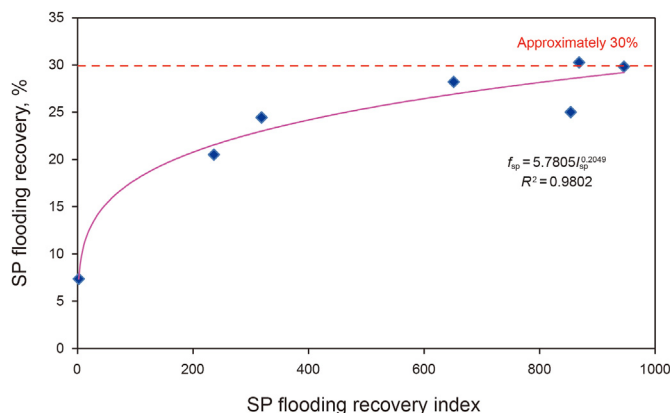


Fig. 13. Crossplot of SP flooding recovery and SP flooding recovery index.

enlarging the sweep volume and improving the oil displacement efficiency. The latter two parameters are the main factors controlling SP flooding recovery. A higher solution viscosity corresponds to a stronger shear force, a lower displacement-liquid phase permeability and a higher oil-phase permeability. Low interfacial tension can reduce the adsorption capacity of the oil phase, and emulsification can further increase the viscosity of the SP solution, which causes the residual oil to be easily isolated and displaced after water flooding. Consequently, the SP flooding recovery is enhanced. Fig. 13 shows that the SP flooding recovery increases with an increased SP flooding recovery index for the seven conglomerate samples. With a constant change in various parameters, the ultimate SP flooding recovery approaches 30%. The calculation formula is as follows:

$$f_{sp} = 5.7805 I_{sp}^{0.2049} \quad (4)$$

$$R^2 = 0.9802$$

where  $f_{sp}$  is the SP flooding recovery, %.

#### 4.4. Application of oil recovery models

Based on the comprehensive analysis of the experimental data from seven natural samples, the main factors influencing the oil recovery of water flooding and SP flooding are identified, and quantitative calculation models of the oil recovery of the conglomerate reservoir under the two displacement modes are established. Combined with reservoir porosity calculated by a logging curve, the average capillary radius determined by core analysis, and the various parameters of the SP solution, this model can calculate the oil recovery of several layers in a single-well control area. Then, the oil recovery values of the whole reservoir in different displacement stages can be calculated by an interpolation simulation algorithm. Table 6 shows the prediction results of water flooding and SP flooding in the Badaowan Formation in the seventh block of the Karamay Oilfield. The water flooding recovery calculated by the seven thin-layer models are 39.7%, 42.7%, 43.9%, 46.6%, 48.7%, 48.1% and 42.8%, respectively. Among them, the main layers of SP flooding, namely, layers  $J_1b_5^{1-1}$  and  $J_1b_5^{1-2}$ , have the highest water flooding recovery values. The cementation type of layer  $J_1b_5^{1-3}$  is mainly calcium cementation, resulting in tight reservoir and low permeability, so the water flooding recovery is low. A comparison of the model calculation results with the actual calibrated water flooding recovery reveals that they have a high degree of agreement and a small average relative error of 4.4%. However, on the whole, the actual calibrated recovery is higher

than that of the model calculation because the model calculation is performed on the premise that the external injection conditions remain unchanged, whereas the reservoir of the Badaowan Formation has undergone the development processes of secondary infilling, well-pattern adjustment and local fracturing. Consequently, the pore structure and flow system in the reservoir have changed in the direction conducive to water flooding, thereby the actual calibrated recovery is enhanced compared with the calculated value.

After water flooding, combined with the residual oil saturation after water flooding and SP solution parameters, the SP flooding recovery is calculated using the established model (Table 6). The calculation results of the seven thin-layer models are 17.5%, 19.4%, 20.5%, 19.7%, 20.7%, 19.1% and 17.2%, respectively. Compared with the results of the numerical simulation, the two methods agree well with each other, and the average relative error is 2.5%. This shows that the calculation accuracy of the SP flooding recovery model is high, which can be promoted and applied in the oilfield. The sum of water flooding recovery and SP flooding recovery is the ultimate oil recovery of the reservoir. According to the calculation results, the ultimate oil recovery of layer  $J_1b_5^{1-1}$  of the Badaowan Formation is the highest, reaching 69.4%, and that of layer  $J_1b_5^{1-2}$  is 67.2%. The cementation type of layer  $J_1b_5^{1-3}$  is mainly calcium cementation, resulting in tight reservoir and low permeability, so the ultimate oil recovery is 60.1%. Due to changes in the sedimentary rhythm and hydrodynamic conditions, the physical properties and pore structure of the reservoir worsen and the ultimate oil recovery and development potential gradually reduce from the bottom layer to the top layer (layers  $J_1b_4^{2-2}$ ,  $J_1b_4^{2-1}$ ,  $J_1b_4^{1-2}$  and  $J_1b_4^{1-1}$ ). The accurate calculation of oil recovery under different displacement modes provides basic data and a geological basis for the reasonable formulation of a SP flooding program.

#### 5. Conclusions

- (1) For conglomerate reservoirs with complex pore structures, there are four types of residual oil after water flooding: oil droplets retained in pore throat by capillary forces, oil cluster trapped at the junction of pores and throats, oil film on the rock surface, isolated oil in dead-ends of flow channel. The formation mechanisms of four types of residual oil are different, and the effective start-up and displacement of these residual oil is the material basis of enhancing SP flooding recovery.
- (2) The oil displacement mechanisms of SP flooding in the studied conglomerate reservoir are primarily controlled by

**Table 6**  
Calculation results of oil recovery of different layers in the Badaowan Formation.

| Layer                          | Porosity calculated by logging, % | Original oil saturation, % | Average capillary radius, $\mu\text{m}$ | Water flooding recovery index | Water flooding recovery, % | Actual calibrated water flooding recovery, % | Residual oil saturation after water flooding, % | SP solution     | Interfacial tension, mN/m | Viscosity of the SP solution, mPa·s | SP flooding recovery index | SP flooding recovery, % | Numerical simulation recovery, % | Ultimate oil recovery, % |
|--------------------------------|-----------------------------------|----------------------------|---|-------------------------------|----------------------------|--|---|-----------------|---------------------------|-------------------------------------|----------------------------|-------------------------|----------------------------------|--------------------------|
| J <sub>164</sub> <sup>-1</sup> | 21.8                              | 62.6                       | 5.29                                    | 15.2                          | 39.7                       | 40.4   | 38.9  | 1500 mg/L       | 0.007                     | 4                                   | 222.3                      | 17.5                    | 18.2                             | 57.2                     |
| J <sub>164</sub> <sup>-2</sup> | 21.7                              | 62.5                       | 6.75                                    | 19.4                          | 42.7                       | 46.3   | 36.5  | HPAM + 0.1% KPS | 0.007                     | 7                                   | 365.0                      | 19.4                    | 19.5                             | 62.0                     |
| J <sub>163</sub> <sup>-1</sup> | 22.2                              | 64.8                       | 7.25                                    | 21.2                          | 43.9                       | 47.2   | 37.4  |                 | 0.007                     | 9                                   | 480.9                      | 20.5                    | 20.1                             | 64.4                     |
| J <sub>164</sub> <sup>-2</sup> | 22.0                              | 64.5                       | 8.54                                    | 25.0                          | 46.6                       | 45.7   | 34.8  |                 | 0.007                     | 8                                   | 397.7                      | 19.7                    | 19.3                             | 66.3                     |
| J <sub>163</sub> <sup>-1</sup> | 21.4                              | 65.5                       | 9.18                                    | 28.1                          | 48.7                       | 51.5   | 35.6  |                 | 0.007                     | 10                                  | 508.6                      | 20.7                    | 21.4                             | 69.4                     |
| J <sub>163</sub> <sup>-2</sup> | 17.6                              | 62.5                       | 7.68                                    | 27.3                          | 48.1                       | 50.7   | 34.1  |                 | 0.007                     | 7                                   | 341.0                      | 19.1                    | 19.6                             | 67.2                     |
| J <sub>163</sub> <sup>-3</sup> | 16.9                              | 60.5                       | 5.49                                    | 19.7                          | 42.8                       | 45.5   | 36.2  |                 | 0.007                     | 4                                   | 206.9                      | 17.2                    | 17.8                             | 60.1                     |

the sweep volume and oil displacement efficiency. Among the four start-up mechanisms of residual oil identified after water flooding, enlarging the sweep volume and improving the oil displacement efficiency are interdependent, but their contributions to enhanced oil recovery are different. For the oil droplets retained in pore throat and isolated oil in dead-ends of flow channel, enlarging the sweep volume is the main way to enhance oil recovery. For the oil cluster trapped at the junction of pores and oil film on the rock surface, improving the oil displacement efficiency is the main way to enhance oil recovery.

- (3) Pore structure is the main internal factor influencing water flooding recovery, while the physical properties and original oil saturation of the reservoir have relatively little influence. The main factor influencing SP flooding recovery is the physical and chemical properties of the solution itself, which primarily control the interfacial tension and solution viscosity in the reservoir. The residual oil saturation after water flooding is the material basis of SP flooding, and its effect on improving oil recovery is second. Based on the analysis of influencing factors, the calculation models of oil recovery under different displacement modes are established. These models can accurately predict the oil recovery during different displacement stages and the ultimate oil recovery of conglomerate reservoirs, thereby providing a geological basis for the efficient development of chemical flooding.

### Acknowledgments

This research was supported by the National Natural Science Foundation of China (No. 41902141), the Fundamental Research Fund for the Central Universities (No. E1E40403) and the Petro-China Innovation Foundation (No. 2018D-5007-0103).

### References

Bai, B.J., Zhou, J., Yin, M.F., 2015. A comprehensive review of polyacrylamide polymer gels for conformance control. *Petrol. Explor. Dev.* 42 (4), 481–487. [https://doi.org/10.1016/S1876-3804\(15\)30045-8](https://doi.org/10.1016/S1876-3804(15)30045-8).

Chen, T., Zhang, G., Ge, J., 2012. Dynamic interfacial tension between Gudaoh heavy oil and petroleum sulfonate/HPAM complex systems. *Petrol. Sci. Technol.* 30 (4), 1417–1423. <https://doi.org/10.1080/10916466.2011.626006>.

Chen, Y.X., Nie, Z.R., 2015. Study on profile control technology of SP binary flooding in conglomerate reservoir, 7<sup>th</sup> block. *Dissertation* (1), 48–50. <https://doi.org/10.3969/j.issn.1003-4609.2015.01.023> (in Chinese).

Dai, C.L., Wang, K., Liu, Y.F., et al., 2015. Reutilization of fracturing flowback fluids in surfactant flooding for enhanced oil recovery. *Energy Fuel.* 29 (4), 2304–2311. <https://doi.org/10.1021/acs.energyfuels.5b00507>.

Deng, S.G., Lv, W.F., Liu, Q.J., et al., 2014. Research on displacement mechanism in conglomerate using CT scanning method. *Petrol. Explor. Dev.* 41 (3), 330–335. <https://doi.org/10.11698/PED.2014.03.08>.

Li, Y.Q., Chen, J.X., Jin, C.Y., et al., 2017. Optimization of SP and ASP flooding after polymer flooding in conglomerate reservoir. *Petrol. Geol. Recov. Effic.* 24 (2), 63–66. <https://doi.org/10.13673/j.cnki.cn37-1359/te.2017.02.010> (in Chinese).

Liu, W.D., Luo, L.T., Liao, G.Z., et al., 2017. Mechanism for enhanced oil recovery of polymer/surfactant binary flooding. *Petrol. Explor. Dev.* 44 (4), 600–607. <https://doi.org/10.11698/PED.2017.04.13>.

Liu, Z.Y., Li, Y.Q., Cui, M.H., et al., 2016. Pore-scale investigation of residual oil displacement in surfactant-polymer flooding using nuclear magnetic resonance experiments. *Petrol. Sci.* 13 (1), 91–99. <https://doi.org/10.1007/s12182-015-0070-5>.

Liu, Z.Y., Li, Y.Q., Leng, R.X., et al., 2020. Effects of pore structure on surfactant/polymer flooding-based enhanced oil recovery in conglomerate reservoirs. *Petrol. Explor. Dev.* 47 (1), 129–139. [https://doi.org/10.1016/S1876-3804\(20\)60012-X](https://doi.org/10.1016/S1876-3804(20)60012-X).

Luo, M.G., Zhang, T.H., 1992. Micropore structure and classification of conglomerate reservoir formation in Karamay oilfield. *Oil Gas Geol.* 13 (2), 201–209. <https://doi.org/10.11743/ogg19920209> (in Chinese).

Olajire, A.A., 2014. Review of ASP EOR (alkaline surfactant polymer enhanced oil recovery) technology in the petroleum industry: prospects and challenges. *Energy* 77, 963–982. <https://doi.org/10.1016/j.energy.2014.09.005>.

Pal, N., Saxena, N., Mandal, A., 2018. Characterization of alkali-surfactant-polymer slugs using synthesized Gemini surfactant for potential application in enhanced oil recovery. *J. Petrol. Sci. Eng.* 168. <https://doi.org/10.1016/>

- [j.petrol.2018.05.026](https://doi.org/10.1016/j.petrol.2018.05.026), 383–300.
- Puerto, M., Hirasaki, G.J., Miller, C.A., et al., 2012. Surfactant systems for EOR in high-temperature, high-salinity environments. *SPE J.* 17 (1), 11–19. <https://doi.org/10.2118/129675-PA>.
- Rogachev, M., Kondrashev, A., 2015. Experiments of fluid diversion ability of a new waterproofing polymer solution. *Petrol. Explor. Dev.* 42 (4), 507–511. [https://doi.org/10.1016/S1876-3804\(15\)30049-5](https://doi.org/10.1016/S1876-3804(15)30049-5).
- Shah, D.O., Schechter, R.S., 1977. Improved Oil Recovery by Surfactant and Polymer Flooding. Academic Press, New York, pp. 25–39. <https://doi.org/10.1016/B978-0-126-41750-0.X5001-4>.
- Sheng, J.J., 2014. A comprehensive review of alkaline-surfactant-polymer (ASP) flooding. *Asia Pac. J. Chem. Eng.* 9 (4), 471–489. <https://doi.org/10.1002/apj.1824>.
- Shiran, B.S., Skauge, A., 2013. Enhanced oil recovery (EOR) by combined low salinity water/polymer injection. *Energy Fuel.* 27 (3), 1223. <https://doi.org/10.1021/ef301538e>.
- Song, H.B., 2014. Research of surfactant-polymer flooding response characteristics and influencing factors: case of Gudong Oilfield. *Nat. Gas Geosci.* 25 (S1), 98–106. <https://doi.org/10.11764/j.issn.1672-1926.2014.S1.0098> (in Chinese).
- Tan, F.Q., Li, H.Q., Xu, C.F., et al., 2010. Quantitative evaluation methods for water-flooded layers of conglomerate reservoir based on well logging data. *Petrol. Sci.* 7 (4), 485–493. <https://doi.org/10.1007/s12182-010-0092-y>.
- Tan, F.Q., Xu, C.F., Zhang, Y.L., et al., 2019. Differences of microscopic seepage mechanisms of water flooding and polymer flooding and prediction models of final oil recovery for conglomerate reservoir. *Oil Gas Sci. Technol.* 74 (13), 1–15. <https://doi.org/10.2516/ogst/2018086>.
- Wang, Y., Peng, J., Zhao, R., 2012. Optimization of SP and ASP flooding after polymer flooding in conglomerate reservoir. *Acta Sedimentol. Sin.* 30 (2), 264–271. <https://doi.org/10.14027/j.cnki.cjxb.2012.02.016> (in Chinese).
- Xu, C.F., Liu, H.X., Qian, G.B., et al., 2011. Microcosmic mechanisms of water-oil displacement in conglomerate reservoirs in Karamay oilfield, NW China. *Petrol. Explor. Dev.* 38 (6), 725–732. [https://doi.org/10.1016/S1876-3804\(12\)60006-8](https://doi.org/10.1016/S1876-3804(12)60006-8).
- Yang, J.Y., Li, Z.Q., Xu, B.H., et al., 2013. Stability and separation of heavy crude SP flooding produced water. *Environ. Sci. Technol.* 36 (10), 7–12. <https://doi.org/10.3969/j.issn.1003-6504.2013.10.002>.
- Zhang, T.K., Zhao, F.L., Hou, J.R., et al., 2010. Research on binary system flooding mechanism under the heterogeneous condition using microscopic model. *Oil Drill. Prod. Technol.* 32 (6), 84–88. <https://doi.org/10.3969/j.issn.1000-7393.2010.06.021> (in Chinese).
- Zhang, L.W., Wang, J., Luan, H.X., et al., 2020. Emulsifying performance and oil displacing test of the surfactant-polymer binary system in conglomerate oil reservoir. *Pet. Geol. Oilfield Dev. Daqing* 39 (6), 112–118. <https://doi.org/10.19597/j.issn.1000-3754.201906017> (in Chinese).